

T-Violation in $K^+ \rightarrow \mu^+ \nu \gamma$ Decay And Supersymmetry

Guo-Hong Wu * and John N. Ng †

TRIUMF Theory Group

4004 Wesbrook Mall, Vancouver, B.C., Canada V6T 2A3

Abstract

Measurement of the transverse muon polarization P_μ^\perp in the $K^+ \rightarrow \mu^+ \nu \gamma$ decay will be attempted for the first time at the ongoing KEK E246 experiment and also at a proposed BNL experiment. We provide a general analysis of how P_μ^\perp is sensitive to the physical CP -violating phases in new physics induced four-Fermi interactions, and then we calculate the dominant contributions to P_μ^\perp from squark family mixings in generic supersymmetric models. Estimates of the upper bounds on P_μ^\perp are also given. It is found that a supersymmetry-induced right-handed quark current from W boson exchange gives an upper limit on P_μ^\perp as large as a few per cent, whereas with charged-Higgs-exchange induced pseudoscalar interaction, P_μ^\perp is no larger than a few tenths of a per cent. Possible correlations between the muon polarization measurements in $K^+ \rightarrow \mu^+ \nu \gamma$ and $K^+ \rightarrow \pi^0 \mu^+ \nu$ decays are discussed, and distinctive patterns of this correlation from squark family-mixings and from the three-Higgs-doublet model are noted.

*gwu@alph02.triumf.ca

†misery@triumf.ca

I. INTRODUCTION

The on-going KEK E246 experiment [1] and a recently proposed BNL experiment [2] are both devoted to testing T -violation to a high precision in the $K^+ \rightarrow \pi^0 \mu^+ \nu$ ($K_{\mu 3}^+$) decay by measuring the transverse muon polarization $P_\mu^{\perp(\pi)} = \mathbf{s}_\mu \cdot (\mathbf{p}_\pi \times \mathbf{p}_\mu) / |\mathbf{p}_\pi \times \mathbf{p}_\mu|$, where \mathbf{p}_π and \mathbf{p}_μ are the momenta of the pion and muon in the kaon rest frame and \mathbf{s}_μ is the muon spin vector. The combined previous measurements [3] at the BNL-AGS constrained the muon polarization to be $P_\mu^{\perp(\pi)} = (-1.85 \pm 3.60) \times 10^{-3}$, and this puts an upper limit of $|P_\mu^{\perp(\pi)}| < 0.9\%$ at the 95% confidence level. The standard model (SM) CP -violating contribution to P_μ^\perp is vanishingly small [4], and the final state interaction (FSI) effect is found to be of order 10^{-6} [5]. Therefore, if an effect is detected at the 10^{-3} level or 10^{-4} level which the KEK experiment and the proposed BNL experiment are respectively sensitive to, it will be an unmistakable signature for new physics. It has been estimated [6] that $P_\mu^{\perp(\pi)}$ can be as large as $\sim 10^{-3}$ in the three-Higgs-doublet model [7]. More recently, we noted that [8] large squark-family-mixings in supersymmetry (SUSY) could contribute to $P_\mu^{\perp(\pi)}$ at the level of 10^{-3} , which is three orders of magnitude larger than that in the absence of squark-family-mixings [9].

The transverse muon polarization, denoted by P_μ^\perp and defined as above with \mathbf{p}_π substituted by the photon momentum \mathbf{p}_γ , will also be measured in the radiative decay mode $K^+ \rightarrow \mu^+ \nu \gamma$ ($K_{\mu 2\gamma}$) both at KEK [1] and at BNL [2]. Here the FSI effect is expected to be large [10], and it could be on the order of 10^{-3} [11]. Being electromagnetic in nature, this effect can be accurately computed and subtracted out. The more interesting standard model CP -violating contribution to P_μ^\perp arising from the Kobayashi-Maskawa (KM) phase [12] is again negligible. The effect of a CP -violating tensor interaction on the muon polarization was considered in Ref. [13]; and the contribution to P_μ^\perp from an effective pseudoscalar four-Fermi operator in the three-Higgs-doublet model (3HDM) has recently been discussed [14]. In this work, we provide a more general analysis of the muon polarization in the $K_{\mu 2\gamma}$ decay by including the complete effective four-Fermi interactions induced from spin-zero

and spin-one boson exchange. Then we concentrate on supersymmetric theories with large squark-generational-mixings where dramatic enhancement effects due to the third family heavy quark masses could give rise to a large P_μ^\perp . Details of this will be given in a later section where SUSY effects are examined.

The outline of the paper is as follows. The framework is laid out in section II for computing P_μ^\perp in $K_{\mu 2\gamma}$ decay in terms of general effective four-Fermi interactions. In section III, we focus on the effects of large squark-family-mixings which are allowed in fairly general SUSY models. Possible correlations of the muon polarization in $K_{\mu 3}$ and $K_{\mu 2\gamma}$ decays are then discussed, and an interesting comparison with multi-Higgs type models is made. The conclusions are presented in section IV.

II. GENERAL FRAMEWORK

Consider the radiative $K_{\mu 2}^+$ decay

$$K^+(p) \rightarrow \gamma(q)\mu^+(l)\nu(p_\nu), \quad (1)$$

where p , q , l and p_ν denote the momenta of the kaon, photon, muon, and neutrino respectively. The SM amplitude for this decay consists of two separately gauge invariant pieces: the inner bremsstrahlung (IB) piece with the photon radiated off the external muon or kaon line, and the structure-dependent (SD) piece for which the photon is emitted from the effective $K\mu\nu$ vertex via some intermediate states. The total amplitude can be written as [15,16],

$$\mathcal{M}_{SM} = \mathcal{M}_{IB} + \mathcal{M}_{SD} \quad (2)$$

$$\mathcal{M}_{IB} = -ie \frac{G_F}{\sqrt{2}} \sin \theta_c f_K m_\mu \epsilon_\alpha^* K^\alpha \quad (3)$$

$$\mathcal{M}_{SD} = ie \frac{G_F}{\sqrt{2}} \sin \theta_c \epsilon_\alpha^* L_\beta H^{\alpha\beta}, \quad (4)$$

with

$$K^\alpha = \bar{u}(p_\nu)(1 + \gamma_5) \left(\frac{p^\alpha}{p \cdot q} - \frac{2l^\alpha + \not{q}\gamma^\alpha}{2l \cdot q} \right) v(l) \quad (5)$$

$$L^\alpha = \bar{u}(p_\nu)\gamma^\alpha(1 - \gamma_5)v(l) \quad (6)$$

$$H^{\alpha\beta} = \frac{F_A}{m_K}(-g^{\alpha\beta}p \cdot q + p^\alpha q^\beta) + i\frac{F_V}{m_K}\epsilon^{\alpha\beta\mu\nu}q_\mu p_\nu, \quad (7)$$

where G_F is the Fermi constant, $\sin\theta_c = 0.22$ is the Cabibbo mixing, m_μ and m_K are the masses of the muon and the kaon, ϵ is the photon polarization vector, f_K is the well determined kaon decay constant, and F_A and F_V are the axial-vector and vector form factors associated with the radiative decay. The kaon decay constant and the two form factors are defined by

$$\langle 0 | \bar{s}\gamma^\mu\gamma_5 u | K^+(p) \rangle = -if_K p^\mu \quad (8)$$

$$\begin{aligned} \int dx e^{iqx} \langle 0 | T(J_{em}^\mu(x) \bar{s}\gamma^\nu\gamma_5 u(0)) | K^+(p) \rangle &= -f_K \left(g^{\mu\nu} + \frac{p^\mu(p-q)^\nu}{p \cdot q} \right) \\ &\quad + \frac{F_A}{m_K} (g^{\mu\nu} p \cdot q - p^\mu q^\nu) \end{aligned} \quad (9)$$

$$\int dx e^{iqx} \langle 0 | T(J_{em}^\mu(x) \bar{s}\gamma^\nu u(0)) | K^+(p) \rangle = i\frac{F_V}{m_K} \epsilon^{\mu\nu\alpha\beta} q_\alpha p_\beta, \quad (10)$$

where $f_K = 160$ MeV, F_A and F_V are functions of $(p-q)^2$, J_{em}^μ is the electromagnetic current, and $\epsilon_{0123} = 1$.

Ideally one would like to be able to extract separately F_V and F_A from experimental data. However, the accuracy of current data does not permit us to do so. On the other hand, various models [17] have been used to calculate the form factors. In chiral perturbation theory at the one-loop level, F_V and F_A are found to be real and are given by [16]

$$F_V = -0.0945 \quad F_A = -0.0425. \quad (11)$$

The momentum dependence of F_V and F_A shows up only at two loops in chiral perturbation theory. Furthermore in the SM, the KM phase will enter the form factors at the two-loop level and hence can be ignored. The above estimate will be used in our analysis of the muon polarization.

As will be shown later, contributions to the $K^+ \rightarrow \mu^+ \nu \gamma$ decay from physics beyond the SM can be parameterized by three dimensionless quantities, δ_{IB} , δ_A and δ_V , to be associated with f_K , F_A , and F_V respectively. The new amplitude is obtained from Eqs. (2)-(7) by the following replacements:

$$f_K \rightarrow f'_K \equiv f_K(1 + \delta_{IB}) \quad (12)$$

$$F_A \rightarrow F'_A \equiv F_A(1 + \delta_A) \quad (13)$$

$$F_V \rightarrow F'_V \equiv F_V(1 + \delta_V) \quad (14)$$

The three δ parameters are in general complex, and could contribute to the T -odd transverse muon polarization P_μ^\perp .

The transverse polarization of the muon in $K^+ \rightarrow \mu^+ \nu \gamma$ decay is defined as

$$P_\mu^\perp = \frac{\mathbf{s}_\mu \cdot (\mathbf{p}_\gamma \times \mathbf{p}_\mu)}{|\mathbf{p}_\gamma \times \mathbf{p}_\mu|}, \quad (15)$$

where \mathbf{s}_μ is the spin vector of the muon, and \mathbf{p}_γ and \mathbf{p}_μ are the three-momenta of the photon and muon. A non-zero P_μ^\perp arises from the interference between the \mathcal{M}_{IB} and \mathcal{M}_{SD} amplitudes. After a general kinematic analysis, we can express P_μ^\perp in the K^+ rest frame as the sum of an IB - F_V interference piece and an IB - F_A interference piece. Explicitly,

$$P_\mu^\perp(x, y) = P_{IB-V}^\perp(x, y) + P_{IB-A}^\perp(x, y) \quad (16)$$

$$P_{IB-V}^\perp(x, y) = \sigma_V(x, y) \text{Im}[(1 + \delta_{IB})(1 + \delta_V^*)] \quad (17)$$

$$P_{IB-A}^\perp(x, y) = \sigma_A(x, y) \text{Im}[(1 + \delta_{IB})(1 + \delta_A^*)], \quad (18)$$

where $x = 2p \cdot q/p^2 = 2E_\gamma/m_K$ and $y = 2p \cdot l/p^2 = 2E_\mu/m_K$ are the normalized energies of the photon and the muon respectively. The functions $\sigma_V(x, y)$ and $\sigma_A(x, y)$ are given by

$$\sigma_V(x, y) = -2\sqrt{r_\mu} \frac{f_K}{m_K} F_V f_V(x, y) \frac{\sqrt{(1-y+r_\mu)((1-x)(x+y-1)-r_\mu)}}{\rho(x, y)} \quad (19)$$

$$\sigma_A(x, y) = -2\sqrt{r_\mu} \frac{f_K}{m_K} F_A f_A(x, y) \frac{\sqrt{(1-y+r_\mu)((1-x)(x+y-1)-r_\mu)}}{\rho(x, y)}, \quad (20)$$

where $r_\mu = m_\mu^2/m_K^2$, $f_V(x, y)$ and $f_A(x, y)$ are to be defined later, and $\rho(x, y) \propto \frac{d\Gamma(K^+ \rightarrow \mu^+ \nu \gamma)}{dx dy}$ is the normalized Dalitz density consisting of the IB piece $\rho_{IB}(x, y)$, the SD piece $\rho_{SD}(x, y)$, and the interference term $\rho_{INT}(x, y)$,

$$\begin{aligned} \rho(x, y) &= \rho_{IB}(x, y) + \rho_{SD}(x, y) + \rho_{INT}(x, y) \\ \rho_{IB}(x, y) &= 2r_\mu \frac{f_K^2}{m_K^2} |1 + \delta_{IB}|^2 f_{IB}(x, y) \\ \rho_{SD}(x, y) &= \frac{1}{2} (|F'_V + F'_A|^2 f_{SD^+}(x, y) + |F'_V - F'_A|^2 f_{SD^-}(x, y)) \\ \rho_{INT}(x, y) &= 2r_\mu \frac{f_K}{m_K} \text{Re}[(1 + \delta_{IB}^*) ((F'_V + F'_A) f_{INT^+}(x, y) + (F'_V - F'_A) f_{INT^-}(x, y))], \end{aligned} \quad (21)$$

with

$$\begin{aligned} f_{IB}(x, y) &= \left(\frac{1 - y + r_\mu}{x^2(x + y - 1 - r_\mu)} \right) \left(x^2 + 2(1 - x)(1 - r_\mu) - \frac{2xr_\mu(1 - r_\mu)}{x + y - 1 - r_\mu} \right) \\ f_{SD^+}(x, y) &= (x + y - 1 - r_\mu)((x + y - 1)(1 - x) - r_\mu) \\ f_{SD^-}(x, y) &= (1 - y + r_\mu)((1 - x)(1 - y) + r_\mu) \\ f_{INT^+}(x, y) &= \left(\frac{1 - y + r_\mu}{x(x + y - 1 - r_\mu)} \right) ((1 - x)(1 - x - y) + r_\mu) \\ f_{INT^-}(x, y) &= \left(\frac{1 - y + r_\mu}{x(x + y - 1 - r_\mu)} \right) (x^2 - (1 - x)(1 - x - y) - r_\mu) \\ f_V(x, y) &= \frac{2 - x - y}{x + y - 1 - r_\mu} \\ f_A(x, y) &= \frac{(2 - x)(x + y) - 2(1 + r_\mu)}{x(x + y - 1 - r_\mu)}. \end{aligned} \quad (22)$$

The next step in the analysis is to compute the δ parameters in Eqs. (12)-(14) in terms of parameters describing the new physics. It is reasonable to assume that at the energies we are considering, new physics can be described by general four-Fermi operators of the form (neglecting possible tensor interactions),

$$\begin{aligned} \mathcal{L} &= -\frac{G_F}{\sqrt{2}} \sin \theta_c \bar{s} \gamma_\alpha (1 - \gamma_5) u \bar{\nu} \gamma^\alpha (1 - \gamma_5) \mu \\ &\quad + G_S \bar{s} u \bar{\nu} (1 + \gamma_5) \mu + G_P \bar{s} \gamma_5 u \bar{\nu} (1 + \gamma_5) \mu \\ &\quad + G_V \bar{s} \gamma_\alpha u \bar{\nu} \gamma^\alpha (1 - \gamma_5) \mu + G_A \bar{s} \gamma_\alpha \gamma_5 u \bar{\nu} \gamma^\alpha (1 - \gamma_5) \mu \\ &\quad + h.c., \end{aligned} \quad (23)$$

where G_S , G_P , G_V and G_A parameterize the non-standard model interactions due to scalar, pseudoscalar, vector and axial-vector boson exchange respectively. In some models, effective right-handed neutrino-muon current can be constructed. Since the SM leptonic charged-current is left-handed, its interference with such a right-handed current will be suppressed by the neutrino mass and will have a negligible contribution to P_μ^\perp . Therefore only left-handed neutrinos need to be considered.

The contributions of the G_S and G_P operators are recently discussed by Kobayashi *et. al.* [14] in the context of the three-Higgs-doublet model, where tree-level charged Higgs exchange is sufficient to give rise to T violation. The relevant hadronic matrix elements involving the scalar current can be related to f_K via [14]

$$\langle 0 | \bar{s} \gamma_5 u | K^+(p) \rangle = i \frac{f_K m_K^2}{m_s + m_u} \quad (24)$$

$$\int dx e^{iqx} \langle 0 | T(J_{em}^\mu(x) \bar{s} \gamma_5 u(0)) | K^+(p) \rangle = \frac{p^\mu}{p \cdot q} \frac{f_K m_K^2}{m_s + m_u} \quad (25)$$

$$\int dx e^{iqx} \langle 0 | T(J_{em}^\mu(x) \bar{s} u(0)) | K^+(p) \rangle = 0 = \langle 0 | \bar{s} u | K^+(p) \rangle. \quad (26)$$

It is immediately seen that the effective scalar interaction (the G_S operator) does not affect the $K_{\mu 2\gamma}$ decay rate as their hadronic matrix elements vanish by parity. On the other hand from Eqs. (24) and (25), the contribution of the G_P operator to the decay amplitude is seen to be non-vanishing and it has the same structure as \mathcal{M}_{IB} of Eq. (3),

$$\mathcal{M}_P = -ieG_P \frac{f_K m_K^2}{m_s + m_u} \epsilon_\alpha^* K^\alpha. \quad (27)$$

This amounts to a contribution to the parameter δ_{IB} only,

$$\delta_{IB}|_{G_P} = \frac{\sqrt{2}G_P}{G_F \sin \theta_c} \frac{m_K^2}{(m_s + m_u)m_\mu}, \quad (28)$$

and the other two parameters, δ_V and δ_A , remain zero.

The effective vector and axial-vector four-Fermi interactions give rise to corrections to the $V - A$ structure of the SM quark current. They can be analyzed by using the

corresponding hadronic matrix elements given by Eqs. (8)-(10). The G_V operator contributes only to δ_V ,

$$\delta_V|_{G_V} = -\frac{\sqrt{2}G_V}{G_F \sin \theta_c}. \quad (29)$$

On the other hand, the axial-vector G_A operator contributes to both δ_{IB} and δ_A ,

$$\delta_{IB}|_{G_A} = \delta_A|_{G_A} = \frac{\sqrt{2}G_A}{G_F \sin \theta_c}. \quad (30)$$

Summing up Eqs. (28)-(30), we obtain the following contributions to the δ parameters from the effective four-Fermi interactions

$$\delta_{IB} = \frac{\sqrt{2}G_P}{G_F \sin \theta_c} \frac{m_K^2}{(m_s + m_u)m_\mu} + \frac{\sqrt{2}G_A}{G_F \sin \theta_c} \quad (31)$$

$$\delta_V = -\frac{\sqrt{2}G_V}{G_F \sin \theta_c} \quad (32)$$

$$\delta_A = \frac{\sqrt{2}G_A}{G_F \sin \theta_c}. \quad (33)$$

As can be seen from Eqs. (16)-(18) and Eqs. (31)-(33), P_μ^\perp in the $K^+ \rightarrow \mu^+\nu\gamma$ decay could receive contributions from the G_P , G_V and G_A effective interactions of Eq. (23). By comparison, $P_\mu^{\perp(\pi)}$ in the $K^+ \rightarrow \pi^0\mu^+\nu$ decay is only sensitive to the G_S interaction [18]. These two decay modes are therefore complementary in searching for new physics effects. As one would expect, if physics beyond the SM has only left-handed quark current, it will not contribute to P_μ^\perp . This can be seen explicitly from Eqs. (31)-(33). For a left-handed quark current ($G_V = -G_A$ and $G_P = G_S = 0$), $\delta_{IB} = \delta_A = \delta_V$, and therefore no relative phase exists between \mathcal{M}_{IB} and \mathcal{M}_{SD} . However, a right-handed quark current as in left-right symmetric models will in general have an effect on P_μ^\perp , and the size of the muon polarization would be model dependent. Signatures of the effective four-Fermi interactions of Eq. (23) for the muon polarization in the $K_{\mu 2\gamma}$ decay are summarized in Table I.

The success of the SM dictates that the magnitudes of the δ parameters of Eqs. (31)-(33) are much smaller than one. We can therefore simplify the formula for P_μ^\perp by neglecting

terms quadratic in the δ 's and by considering only the relevant G_P and G_R interactions given by

$$\Delta\mathcal{L} = G_P \bar{s} \gamma_5 u \bar{\nu} (1 + \gamma_5) \mu + G_R \bar{s} \gamma_\alpha (1 + \gamma_5) u \bar{\nu} \gamma^\alpha (1 - \gamma_5) \mu + h.c.. \quad (34)$$

Combining Eqs. (16)-(18) and (31)-(33), the muon transverse polarization can be rewritten as a sum of the G_P interaction contribution $P_{\mu,P}^\perp(x, y)$ and the G_R interaction contribution $P_{\mu,R}^\perp(x, y)$,

$$P_\mu^\perp(x, y) = P_{\mu,P}^\perp(x, y) + P_{\mu,R}^\perp(x, y) \quad (35)$$

$$P_{\mu,P}^\perp(x, y) = \sigma(x, y) \text{Im} \Delta_P \quad (36)$$

$$P_{\mu,R}^\perp(x, y) = 2\sigma_V(x, y) \text{Im} \Delta_R, \quad (37)$$

where

$$\sigma(x, y) = \sigma_V(x, y) + \sigma_A(x, y) \quad (38)$$

$$\Delta_P \equiv \frac{\sqrt{2} G_P}{G_F \sin \theta_c} \frac{m_K^2}{(m_s + m_u) m_\mu} \quad (39)$$

$$\Delta_R \equiv \frac{\sqrt{2} G_R}{G_F \sin \theta_c}. \quad (40)$$

The contour plots of $\rho(x, y)$, $\sigma(x, y)$, $\sigma_V(x, y)$, and $\sigma_A(x, y)$ are given in Fig. 1. The infrared sensitivity of the $K_{\mu 2\gamma}$ decay rate manifests itself in the Dalitz plot $\rho(x, y)$ in the soft photon (i.e. small x) region.

Due to the experimental necessity of cutting out low energy photons, it is more useful to define the quantity \overline{P}_μ^\perp by

$$\overline{P}_\mu^\perp \equiv \frac{\int_S dx dy \rho(x, y) P_\mu^\perp(x, y)}{\int_S dx dy \rho(x, y)}, \quad (41)$$

which is the average of $P_\mu^\perp(x, y)$ over a region of phase space S . In this definition, the numerator measures the difference in number in the region S between muons pointing their spin vector along the direction $\mathbf{p}_\gamma \times \mathbf{p}_\mu$ and those along the opposite direction, and the

denominator is a measure of the total number of muons in the region S . In terms of the effective four-Fermi interactions, the average muon polarization is given by

$$\overline{P}_\mu^\perp = \overline{P}_{\mu,P}^\perp + \overline{P}_{\mu,R}^\perp = \overline{\sigma}Im\Delta_P + 2\overline{\sigma_V}Im\Delta_R. \quad (42)$$

Plots of the averaged $\overline{\sigma}$, $\overline{\sigma_V}$ and $-\overline{\sigma_A}$ as a function of the energy cut on soft photons are given in Fig. 2. The typical size of $\overline{\sigma}$ and $\overline{\sigma_V}$ for the $K_{\mu 2\gamma}^+$ decay can be seen to be of order 0.1, and it is a kinematic measure of the relative strength of the \mathcal{M}_{IB} - \mathcal{M}_{SD} interference and the IB plus SD contributions to the partial width. The corresponding values for the radiative decays of $\pi^+ \rightarrow \mu^+\nu\gamma$ ($\pi_{\mu 2\gamma}$) and $K^+ \rightarrow e^+\nu\gamma$ ($K_{e 2\gamma}$) are expected to be roughly two orders of magnitude smaller than for $K_{\mu 2\gamma}$ decay because of the dominance of the IB and SD contributions respectively. And this makes it difficult to measure the transverse lepton polarization in the $\pi_{\mu 2\gamma}$ and $K_{e 2\gamma}$ modes.

III. SUSY EFFECTS

In the minimal supersymmetric standard model (MSSM, by this we mean with minimal particle content and with R -parity conservation), T -violation in $K^+ \rightarrow \mu^+\nu\gamma$ decay arises from the interference between the SM tree amplitude and the one-loop MSSM amplitude. Naively, this would be suppressed at least by α_s/π (α_s is the QCD coupling) relative to the tree level interference effect as in the three-Higgs-doublet model [14], and would be too small to be seen. However, this would not be the case when the squark family mixings are taken into account. Then T -violation in $K_{\mu 2\gamma}$ decay could be sensitive to the top and bottom quarks of the third family, and large enhancement effects due to the heavy quark masses could appear [8]. This scenario will be the focus of our attention in the discussion of the SUSY contributions to the muon polarization.

The notion of squark family mixings comes from the general assumption that the mass matrices of the quarks and squarks are diagonalized by different unitary transformations

in generation space [19]. In principle, these mixing matrices could all be determined in specific models. In the lack of a generally accepted SUSY flavor model, we adopt a model-independent approach and refer interested readers to the literature for discussions of specific models [20,21]. The relative rotations in generation space between the \tilde{u}_L , \tilde{u}_R , \tilde{d}_L , and \tilde{d}_R squarks and their corresponding quark partners are denoted by V^{UL} , V^{UR} , V^{DL} , and V^{DR} respectively. These matrices appear in the quark-squark-gluino couplings which lead to new contributions to flavor-changing neutral current processes (FCNC) [19]. Meanwhile, these generational mixing matrices give rise to the interesting possibility that the heavy fermions of the third family may play an important role in low energy processes, including the neutron electric dipole moment [22].

As FCNC processes occur only at loop level in both the SM and the MSSM, severe constraints on the squark family mixings can be derived [19] based on available experimental data. For charged-current (CC) processes on the other hand, the SM contributions often appear at tree level whereas effects of squark family mixings arise only at loop-level, and current data in the hadronic sector are not precise enough to put useful bounds on the squark mixing matrices. The FCNC constraints can be written in the form of upper limits either on product of different V^D 's, as from $K\bar{K}$ and $B\bar{B}$ systems and from $b \rightarrow s\gamma$, or on product of different V^U 's, as from $D\bar{D}$ mixing. Without assumptions on or model preference for these mixing matrices, the individual matrix element can however still be of order one.

Charged-current processes involve the product of V^U and V^D , and the size of both mixing matrix elements can be of order one without violating the FCNC bounds. Because of the large top Yukawa coupling, sizable squark mixings with the third generation could then lead to large enhancement effects in low energy charged-current processes. Although this loop-level enhancement may not have significant effects on CP -conserving, tree-level CC processes, it could have dramatic consequences for CP -violating CC processes for which the standard model effects are negligible. This possibility has recently been discussed in the context of T violation in charged meson semileptonic decays [8]. In this work, we would like

to extend the analysis to the transverse muon polarization in the radiative $K_{\mu 2}$ decay.

The physical phases that are relevant for the transverse muon polarization could come from both the squark mixing matrices and other soft SUSY breaking operators including the A terms and the gaugino mass terms. For the sake of simplicity and a clearer illustration of the underlying physics, we concentrate on the phases in the squark mixing matrices. Mass-insertion approximation will be used for the $\tilde{t}_L\text{-}\tilde{t}_R$ and $\tilde{b}_L\text{-}\tilde{b}_R$ mixings, and $m_{\tilde{t}_L} = m_{\tilde{t}_R} = m_{\tilde{t}}$ and $m_{\tilde{b}_L} = m_{\tilde{b}_R} = m_{\tilde{b}}$ will be assumed for the mass parameters of the left and right top and bottom squarks. With large generational squark mixings, the dominating contributions to P_μ^\perp are expected to come from the G_P and G_R four-Fermi operators induced by the $\tilde{t}\text{-}\tilde{b}\text{-}\tilde{g}$ loop diagrams with W boson and charged Higgs boson exchange. The muon polarization will then be directly proportional to $|V_{31}^{U,L,R}V_{32}^{D,L,R*}|$.

A. W Exchange

An effective right-handed current interaction $W^\mu\overline{s}_R\gamma_\mu u_R$ can be generated by the diagram with $\tilde{g}\text{-}\tilde{t}\text{-}\tilde{b}$ sparticles in the loop and with $\tilde{t}_L\text{-}\tilde{t}_R$ and $\tilde{b}_L\text{-}\tilde{b}_R$ mass insertions (see Fig. 3(a)). This gives rise to an effective G_R interaction,

$$\mathcal{L}_1 = -\frac{4G_F}{\sqrt{2}}C_0(\overline{s}_R\gamma^\alpha u_R)(\overline{\nu}_L\gamma_\alpha\mu_L) + h.c. \quad (43)$$

with

$$C_0 = \frac{\alpha_s}{36\pi}I_0\frac{m_t m_b(A_t - \mu \cot\beta)(A_b - \mu \tan\beta)}{m_{\tilde{g}}^4}V_{33}^{SKM*}V_{31}^{UR}V_{32}^{DR*}, \quad (44)$$

where $\alpha_s \simeq 0.1$ is the QCD coupling evaluated at the mass scale of the sparticles in the loop, A_t and A_b are the soft SUSY breaking A terms for the top and bottom squarks, μ denotes the two Higgs superfields mixing parameter, $\tan\beta$ is the ratio of the two Higgs VEVs, $m_{\tilde{g}}$ is the mass of the gluino, V_{ij}^{SKM} is the super KM matrix associated with the W -squark coupling $W^+\tilde{u}_{iL}^*\tilde{d}_{jL}$, and the integral function I_0 is given by

$$I_0 = \int_0^1 dz_1 \int_0^{1-z_1} dz_2 \frac{24z_1z_2}{\left[\frac{m_{\tilde{t}}^2}{m_{\tilde{g}}^2}z_1 + \frac{m_{\tilde{b}}^2}{m_{\tilde{g}}^2}z_2 + (1 - z_1 - z_2)\right]^2}. \quad (45)$$

Note that $I_0 = 1$ for $\frac{m_{\tilde{t}}}{m_{\tilde{g}}} = \frac{m_{\tilde{b}}}{m_{\tilde{g}}} = 1$, but it increases rapidly to ~ 8 as the squark-to-gluino mass ratios decrease to $\frac{m_{\tilde{t}}}{m_{\tilde{g}}} = \frac{m_{\tilde{b}}}{m_{\tilde{g}}} = \frac{1}{2}$. For the case of $m_{\tilde{t}} = m_{\tilde{b}}$, the variation of I_0 with the mass ratio is plotted in Fig. 4.

From Eqs. (43)-(44) and Eq. (40), the right-handed current contribution to Δ_R is found to be

$$\Delta_R|_{\mathcal{L}_1} = -\frac{\alpha_s}{36\pi} I_0 \frac{m_{\tilde{t}} m_b (A_t - \mu \cot \beta) (A_b - \mu \tan \beta)}{m_{\tilde{g}}^4} \times \frac{[V_{33}^{SKM*} V_{31}^{UR} V_{32}^{DR*}]}{\sin \theta_c}. \quad (46)$$

Later on, this will be used to estimate the size of the muon polarization from W -exchange-induced G_R interaction.

An effective pseudo-scalar four-Fermi interaction can be induced at one-loop by invoking a $\tilde{t}_L\text{-}\tilde{t}_R$ insertion (see Fig. 3(b)). To linear order in the external momenta, the W -exchange diagram gives [8]

$$\mathcal{L}_2 = \frac{4G_F}{\sqrt{2}} \left[\frac{C_1}{m_s} (p_s - p_u)^\alpha + \frac{C_2}{m_\mu} (p_s + p_u)^\alpha \right] (\bar{s}_L u_R) (\bar{\nu}_L \gamma_\alpha \mu_L) + h.c., \quad (47)$$

where p_s and p_u are the momenta of the s and u quarks respectively, and $C_{1,2}$ are given by

$$C_1 = \frac{\alpha_s}{36\pi} I_1 \frac{m_s m_t (A_t - \mu \cot \beta)}{m_{\tilde{g}}^3} V_{33}^{SKM*} V_{32}^{DL*} V_{31}^{UR} \quad (48)$$

$$C_2 = \frac{\alpha_s}{36\pi} I_2 \frac{m_\mu m_t (A_t - \mu \cot \beta)}{m_{\tilde{g}}^3} V_{33}^{SKM*} V_{32}^{DL*} V_{31}^{UR}, \quad (49)$$

with

$$I_1 = \int_0^1 dz_1 \int_0^{1-z_1} dz_2 \frac{24z_1(1 - z_1 - z_2)}{\left[\frac{m_{\tilde{t}}^2}{m_{\tilde{g}}^2}z_1 + \frac{m_{\tilde{b}}^2}{m_{\tilde{g}}^2}z_2 + (1 - z_1 - z_2)\right]^2} \quad (50)$$

$$I_2 = \int_0^1 dz_1 \int_0^{1-z_1} dz_2 \frac{24z_1(z_1 - z_2)}{\left[\frac{m_{\tilde{t}}^2}{m_{\tilde{g}}^2}z_1 + \frac{m_{\tilde{b}}^2}{m_{\tilde{g}}^2}z_2 + (1 - z_1 - z_2)\right]^2}. \quad (51)$$

Both integrals $I_{1,2}$ are equal to one at $\frac{m_{\tilde{t}}}{m_{\tilde{g}}} = \frac{m_{\tilde{b}}}{m_{\tilde{g}}} = 1$, and both increase as $\frac{m_{\tilde{t}}}{m_{\tilde{g}}}$ and/or $\frac{m_{\tilde{b}}}{m_{\tilde{g}}}$ decreases from one. For example, $I_1 \sim 4$ and $I_2 \sim 8$ when $\frac{m_{\tilde{t}}}{m_{\tilde{g}}} = \frac{m_{\tilde{b}}}{m_{\tilde{g}}} = \frac{1}{2}$. The functions I_1 and I_2 are plotted in Fig. 4 for the case $m_{\tilde{t}} = m_{\tilde{b}}$.

Notice that the C_2 term in Eq. (47) can be rewritten as an effective scalar interaction by use of the Dirac equation for the external leptons. The term $(p_s - p_u)^\alpha (\bar{s}_L u_R)$ in Eq. (47) can be Gordon decomposed into a tensor piece, a left-handed current piece, and a right-handed current piece. The tensor piece can be neglected as the tensor form factor is expected to be small ¹. The left-handed piece, having the same structure as the standard model interaction, does not contribute to P_μ^\perp (see Table I). The relevant operators of the effective lagrangian \mathcal{L}_2 can thus be rewritten as

$$\mathcal{L}_2 = -\frac{4G_F}{\sqrt{2}} C_1 (\bar{s}_R \gamma^\alpha u_R) (\bar{\nu}_L \gamma_\alpha \mu_L) - \frac{4G_F}{\sqrt{2}} C_2 (\bar{s}_L u_R) (\bar{\nu}_L \mu_R) + \dots, \quad (52)$$

where C_1 and C_2 measure the strengths of the induced G_R and G_P interactions respectively.

The \mathcal{L}_2 contribution to Δ_R and Δ_P can be read off from Eqs. (52,40,39),

$$\Delta_R|_{\mathcal{L}_2} = -\frac{\alpha_s}{36\pi} I_1 \frac{m_s m_t (A_t - \mu \cot \beta)}{m_g^3} \times \frac{[V_{33}^{SKM*} V_{32}^{DL*} V_{31}^{UR}]}{\sin \theta_c} \quad (53)$$

$$\Delta_P|_{\mathcal{L}_2} = -\frac{\alpha_s}{36\pi} I_2 \frac{m_K}{(m_s + m_u)} \times \frac{m_K m_t (A_t - \mu \cot \beta)}{m_g^3} \times \frac{[V_{33}^{SKM*} V_{32}^{DL*} V_{31}^{UR}]}{\sin \theta_c}. \quad (54)$$

It is readily seen that $\Delta_R|_{\mathcal{L}_2}$ is suppressed relative to $\Delta_R|_{\mathcal{L}_1}$ at least by a factor of $m_b/m_s \sim 30$ and will not be considered. By taking the sparticle masses to be about 100 GeV and assuming maximal squark family mixings, the size of $\Delta_P|_{\mathcal{L}_2}$ is found to be at most of order 10^{-4} , and thus the contribution to the averaged transverse muon polarization is at best of order 10^{-5} . For these reasons, the effective lagrangian \mathcal{L}_2 will not be considered further.

We note in passing that a $\tilde{b}_L - \tilde{b}_R$ insertion in a diagram similar to Fig. 3(b) can also induce effective G_R and G_P interactions analogous in form to Eqs. (52)-(54). However, Δ_R will be suppressed by $\frac{m_u m_b}{m_s m_t} \sim 10^{-3}$ relative to that of Eq. (53), whereas the induced Δ_P can at most be comparable to that of Eq. (54) in the large $\tan \beta$ limit when the left-right mixings in the top and bottom squarks could be of the same order of magnitude. Their contributions to the muon polarization are also negligible.

¹See however Ref. [13] for a discussion of tensor effects.

In contrast to $\Delta_R|_{\mathcal{L}_2}$ and $\Delta_P|_{\mathcal{L}_2}$, the magnitude of $\Delta_R|_{\mathcal{L}_1}$ can be enhanced by a large $\tan\beta$. The present data constrains $\tan\beta/m_H < 0.52 \text{ GeV}^{-1}$ [23], where m_H is the mass of the charged Higgs boson. For $m_H = 100 \text{ GeV}$, we can take $\tan\beta = 50$. The muon polarization also depends on the squark mixings $|V_{32}^{D_L}|$ and $|V_{31}^{U_R}|$ (taking $|V_{33}^{SKM}| \sim 1$). As pointed out earlier, the $V^{U'}$'s are constrained by $D\bar{D}$ mixing only in the product of $V_{31}^{U_{L,R}}$ and $V_{32}^{U_{L,R}}$, and $|V_{31}^{U_R}| = \mathcal{O}(1)$ is still allowed. On the other hand, if assuming $|V_{33}^D| = \mathcal{O}(1)$, the FCNC process $b \rightarrow s\gamma$ can put a bound on $|V_{32}^D|$ from the gluino diagram. However, other SUSY contributions to $b \rightarrow s\gamma$, including the charged Higgs and chargino contributions [24], can dominate over the gluino effect and render the bound on $|V_{32}^D|$ meaningless. This is particularly true if the chargino is relatively light.

Recall that the integral I_0 can be of order 10 for reasonable mass ratios of the squarks and gluinos. To estimate the maximal size of $\Delta_R|_{\mathcal{L}_1}$, we therefore take $I_0 = 10$, $\tan\beta = 50$, $A_t = A_b = |\mu| = m_{\tilde{g}} = 100 \text{ GeV}$, and $|V_{31}^{U_R}| = |V_{32}^{D_R}| = \frac{\sqrt{2}}{2}$ for maximal squark family mixings. Then we have for its magnitude

$$\Delta_R|_{\mathcal{L}_1} \leq 0.01 I_0 \leq 0.1. \quad (55)$$

Depending on the soft photon energy cut, it is seen from Fig. 2 that averaging over phase space gives $\bar{\sigma}$ in the 0 – 0.11 range, whereas $\overline{\sigma_V}$ takes values between 0 and 0.17. For an estimate, we choose $E_\gamma^{cut} = 120 \text{ MeV}$, for which $\bar{\sigma} \simeq 0.1$ and $2\overline{\sigma_V} \simeq 0.3$. The magnitude of the average muon polarization from the W -induced effective G_R interaction is then

$$\overline{P_\mu^\perp}|_{\mathcal{L}_1} \simeq 2\overline{\sigma_V} \text{Im}\Delta_R|_{\mathcal{L}_1} < 3 \times 10^{-2}. \quad (56)$$

This limit scales as $\left(\frac{100 \text{ GeV}}{M_{SUSY}}\right)^2 \left(\frac{\tan\beta}{50}\right) \left(\frac{I_0}{10}\right) \left(\frac{\text{Im}[V_{33}^{SKM*} V_{31}^{U_R} V_{32}^{D_R*}]}{0.5}\right)$, where M_{SUSY} is the SUSY breaking scale.

B. H^+ Exchange

By using the Dirac equation and Lorentz invariance of the amplitude, it can be seen that charged Higgs exchange only gives rise to G_P but not G_R interactions. The m_t -enhanced effective four-Fermi interaction is obtained from the diagram that contains a \tilde{g} - \tilde{t} - \tilde{b} loop and the $H^-\tilde{t}_R\tilde{b}_L^*$ vertex (see Fig. 3(c)). It is given by [8]

$$\mathcal{L}_H = \frac{4G_F}{\sqrt{2}}C_H(\bar{s}_L u_R)(\bar{\nu}_L \mu_R) + h.c., \quad (57)$$

with

$$C_H = -\frac{\alpha_s}{3\pi}I_H \tan\beta \frac{m_t m_\mu \mu + A_t \cot\beta}{m_H^2} V_{33}^{H*} V_{32}^{DL*} V_{31}^{UR}, \quad (58)$$

where V_{ij}^H is the mixing matrix in the charged-Higgs-squark coupling $H^+ \tilde{u}_{iR}^* \tilde{d}_{jL}$, and where the integral function I_H is given by

$$I_H = \int_0^1 dz_1 \int_0^{1-z_1} dz_2 \frac{2}{\frac{m_{\tilde{t}}^2}{m_{\tilde{g}}^2} z_1 + \frac{m_{\tilde{b}}^2}{m_{\tilde{g}}^2} z_2 + (1 - z_1 - z_2)}, \quad (59)$$

which is equal to one at $m_{\tilde{t}} = m_{\tilde{b}} = m_{\tilde{g}}$. The function I_H is plotted in Fig. 4 for the case of $m_{\tilde{t}} = m_{\tilde{b}}$. It is seen from the figure that I_H increases relatively slowly to 2.3 as $m_{\tilde{t}}$ and $m_{\tilde{b}}$ decrease to half the gluino mass. The contribution to Δ_P from charged Higgs exchange is given as,

$$\Delta_P|_{\mathcal{L}_H} = -\frac{\alpha_s}{3\pi}I_H \tan\beta \frac{m_K}{(m_s + m_u)} \frac{m_K m_t}{m_H^2} \times \frac{\mu + A_t \cot\beta}{m_{\tilde{g}}} \times \frac{[V_{33}^{H*} V_{32}^{DL*} V_{31}^{UR}]}{\sin\theta_c}. \quad (60)$$

To estimate the upper limit on P_μ^\perp from Higgs boson exchange, we assume maximal squark mixings with $|V_{32}^{DL}| = |V_{31}^{UR}| = 1/\sqrt{2}$ and take $|V_{33}^H| \sim 1$, $m_H = 100$ GeV and $\tan\beta = 50$. Setting $|\mu| = A_t = m_{\tilde{g}}$, $m_s = 150$ MeV, and $I_H = 1$, we find $|\Delta_P|_{\mathcal{L}_H} \leq 0.03$. For $E_\gamma^{cut} = 120$ MeV, the magnitude of the average muon polarization is then

$$\overline{P_\mu^\perp}|_{\mathcal{L}_H} \simeq 0.1 I m \Delta_P|_{\mathcal{L}_H} \leq 3 \times 10^{-3}. \quad (61)$$

This limit scales as $\left(\frac{100 \text{ GeV}}{m_H}\right)^2 \frac{\tan\beta}{50} \frac{\text{Im}[V_{33}^{H*} V_{32}^{DL*} V_{31}^{UR}]}{0.5}$.

It should be noted that the diagram involving the $H^- \tilde{t}_L \tilde{b}_R^*$ coupling is proportional to different squark mixing matrices than those appearing in Eq. (58), and that it is suppressed by m_b . To be explicit, the induced four-Fermi operator is of the form

$$\mathcal{L}_{H,m_b} = \frac{4G_F}{\sqrt{2}} C_{H,m_b} (\bar{\nu}_R u_L) (\bar{\nu}_L \mu_R) + h.c., \quad (62)$$

with

$$C_{H,m_b} = -\frac{\alpha_s}{3\pi} I_H \tan\beta \frac{m_b m_\mu \mu + A_b \tan\beta}{m_H^2} \frac{1}{m_{\tilde{g}}} V_{33}^{\mathcal{H}*} V_{32}^{DR*} V_{31}^{UL}, \quad (63)$$

where $V_{ij}^{\mathcal{H}}$ denotes the mixing matrix in the charged-Higgs-squark coupling $H^+ \tilde{u}_i^* \tilde{d}_j^*$.

In the large $\tan\beta$ limit however, the magnitude of C_{H,m_b} may be as large as that of C_H ,

$$\frac{C_{H,m_b}}{C_H} = \frac{m_b(\mu + A_b \tan\beta)}{m_t(\mu + A_t \cot\beta)} \frac{V_{32}^{DR*} V_{31}^{UL}}{V_{32}^{DL*} V_{31}^{UR}} \simeq \frac{m_b \tan\beta}{m_t} \frac{A_b}{\mu} \frac{V_{32}^{DR*} V_{31}^{UL}}{V_{32}^{DL*} V_{31}^{UR}}, \quad (64)$$

where we have taken $V_{33}^{\mathcal{H}} = V_{33}^H = \mathcal{O}(1)$. Assume $|V_{32}^{DR*} V_{31}^{UL}| \simeq |V_{32}^{DL*} V_{31}^{UR}|$ and $A_b \simeq |\mu|$, then $|C_{H,m_b}| \sim |C_H|$ when $\tan\beta \simeq m_t/m_b$. Within this region of the parameter space, the contribution to P_μ^\perp from the effective interaction of Eq. (62) can be comparable to the m_t -enhanced effect of Eq. (61). However, the maximal size of P_μ^\perp is not expected to be significantly modified.

C. Discussions

Several remarks concerning the effective right-handed current contribution $\Delta_R|_{\mathcal{L}_1}$ of Eq. (46) and the effective pseudoscalar contribution $\Delta_P|_{\mathcal{L}_H}$ of Eq. (60) are in order. As noted before, an effective G_R operator can be induced by W boson exchange only, whereas the G_P interaction can arise from both the W and charged Higgs boson exchange. However, the W -induced G_P interaction never gives a large contribution to P_μ^\perp (see Eq. (54)). In

contrast, both the W -induced G_R operator (Eqs. (43)-(44)) and the charged Higgs induced G_P operator (Eqs. (57)-(58)) are enhanced in the large $\tan\beta$ limit, and large contributions to the muon polarization are found to be possible.

Firstly, the enhancement effects due to squark family mixings are readily seen from Eqs. (46) and (60). Without squark family mixings, Δ_R will be suppressed by a factor of $\frac{m_s m_u}{m_t m_b} \simeq 10^{-6}$ relative to the result of Eq. (46), and would make the effective right-handed current effect totally uninteresting. Similarly, Δ_P of Eq. (60) would be subject to a suppression factor of $\frac{m_s m_\mu}{m_t m_\mu} = \frac{m_s}{m_t} \simeq 10^{-3}$ in the absence of squark flavor mixings.

Secondly, the different dependence of $\Delta_R|_{\mathcal{L}_1}$ (Eq. (46)) and $\Delta_P|_{\mathcal{L}_H}$ (Eq. (60)) on the SUSY parameters is to be noted. On one hand, $\Delta_R|_{\mathcal{L}_1}$ involves V_{32}^{DR*} whereas $\Delta_P|_{\mathcal{L}_H}$ is proportional to V_{32}^{DL*} , and different models of flavor physics could have very different predictions for these two squark family mixing elements. On the other hand, $\Delta_R|_{\mathcal{L}_1} \propto 1/M_{SUSY}^2$ and $\Delta_P|_{\mathcal{L}_H} \propto 1/m_H^2$. Depending on the the scales of M_{SUSY} and m_H , either the W exchange or charged Higgs exchange can give the leading contribution to P_μ^\perp .

If however assuming $|V_{32}^{DR}| = |V_{32}^{DL}|$ and $M_{SUSY} = m_H$, the effective G_R and G_P operators contribute quite differently to P_μ^\perp because of their different chirality structures. As can be seen from Eqs. (44) and (58), $G_R \propto m_t m_b$ and $G_P \propto m_t m_\mu$, and therefore $G_R/G_P \sim m_b/m_\mu \sim 50$. This difference in strength is due to the fact that Yukawa couplings are proportional to the fermion masses whereas gauge interactions are not subject to light fermion mass suppression. We recall that the m_t and m_b factors in G_R come from left-right mixings in the top and bottom squark propagators. To estimate the relative contributions to P_μ^\perp from G_R and G_P , we use Eqs. (36) and (37),

$$\frac{|P_{\mu,R}^\perp|}{|P_{\mu,P}^\perp|} = \frac{2\sigma_V}{\sigma} \frac{(m_s + m_u)m_\mu}{m_K^2} \frac{|ImG_R|}{|ImG_P|} \simeq \frac{1}{5} \frac{m_b}{m_\mu} \frac{I_0}{10} \simeq 1 - 10 \quad (65)$$

where the value $\frac{2\sigma_V}{\sigma} = 3$ has been used, $I_0 = 1 - 10$ (see Fig. 4), and we have assumed the same magnitude for the phases of G_R and G_P . This ratio estimate is not sensitive to the value of $\tan\beta$, and for $I_0 = 10$ it agrees with our more detailed calculations of Eqs. (56) and

(61).

Our third remark concerns the loop suppression factor α_s/π and the enhancement effects due to heavy quarks. For this purpose, it is interesting to compare the SUSY loop contribution and the tree level contribution in the three Higgs doublet model (3HDM) [14]. Assuming maximal squark family mixings and neglecting factors associated with ratios of the Higgs VEVs, we have for SUSY charged Higgs exchange

$$\frac{|P_{\mu,P}^\perp|}{|P_{3HDM}^\perp|} \sim \frac{\alpha_s}{3\pi} \frac{m_t m_\mu}{m_s m_\mu} \sim 10, \quad (66)$$

and for SUSY W -exchange

$$\frac{|P_{\mu,R}^\perp|}{|P_{3HDM}^\perp|} \sim \frac{1}{5} \frac{\alpha_s}{36\pi} I_0 \frac{m_t m_b}{m_s m_\mu} \frac{m_H^2}{M_{SUSY}^2} \sim (10 - 10^2) \times \frac{m_H^2}{M_{SUSY}^2} \quad (\text{for } I_0 = 1 - 10), \quad (67)$$

where P_{3HDM}^\perp is the muon polarization in the 3HDM, and where the prefactor of $\frac{1}{5}$ comes from Eq. (65) and it accounts for the difference in the hadronic matrix elements and kinematic factors between the G_P and G_R interactions. Note that $\frac{P_{\mu,R}^\perp}{P_{3HDM}^\perp} \propto \frac{m_H^2}{M_{SUSY}^2}$, and this ratio can be suppressed if the SUSY breaking scale is much higher than the charged Higgs mass. Therefore in the presence of large squark generational mixings, the heavy quark enhancement effects can overcome the loop suppression and the SUSY contribution to P_μ^\perp could be larger than the 3HDM tree-level contribution by one or two orders of magnitude.

The fourth and final remark concerns possible correlations of the muon polarization between the $K_{\mu 3}$ decay and the $K_{\mu 2\gamma}$ decay.

We first consider charged-Higgs-exchange effects. For both $K_{\mu 3}$ and $K_{\mu 2\gamma}$ decays, the dominant contribution to the muon polarization could come respectively from the scalar and pseudoscalar components of the m_t -enhanced effective operator of Eq. (57). It is therefore expected that charged Higgs contribution to the muon polarization is comparable for both decays, as confirmed by the explicit calculations of Eq. (61) for the $K_{\mu 2\gamma}$ decay and of Ref. [8] for the $K_{\mu 3}$ decay. Since $G_S = G_P$ from Eq. (57), it is found that the average muon polarization in $K_{\mu 3}$ decay is about a factor of 2 bigger than in $K_{\mu 2\gamma}$ decay, but with opposite

sign ². It is interesting to compare our results with the analysis by Kobayashi *et. al.* [14] in the 3HDM. Since the charged Higgs coupling to light quarks is suppressed by the quark masses, the dominating four-fermion operator arising from tree level charged Higgs exchange in the 3HDM is expected to be of the form $(\bar{s}_R u_L)(\bar{\nu}_L \mu_R)$. Therefore, $G_S = -G_P$ in the 3HDM and the muon polarization has the same sign for $K_{\mu 3}$ and $K_{\mu 2\gamma}$ decays. This sign difference is useful for distinguishing between the 3HDM and the SUSY-induced interaction in Eq. (57).

If however, the W -exchange-induced G_R interaction dominates over the charged Higgs-induced G_P (and G_S) interaction as we have argued on general grounds, P_μ^\perp in $K_{\mu 2\gamma}$ decay can be much larger than $P_\mu^{\perp(\pi)}$ in $K_{\mu 3}$ decay. In this case, different squark mixing matrices are involved in these two decays and the relative sign of the muon polarization can not be predicted. Such a large difference in the magnitude of the muon polarization between the $K_{\mu 2\gamma}$ and $K_{\mu 3}$ decays is a special feature of squark-family mixing and does not occur in the 3HDM.

IV. CONCLUSION

As discussed before, the transverse muon polarization $P_\mu^{\perp(\pi)}$ in the $K^+ \rightarrow \pi^0 \mu^+ \nu$ ($K_{\mu 3}$) decay is sensitive to an effective scalar interaction, whereas P_μ^\perp in the $K^+ \rightarrow \mu^+ \nu \gamma$ ($K_{\mu 2\gamma}$) decay can receive contributions from effective pseudoscalar, vector, and axial-vector four-Fermi interactions. Due to the V-A nature of the standard model charged-current, only pseudoscalar (G_P) and right-handed current (G_R) interactions of Eq. (34) contribute to P_μ^\perp in the $K_{\mu 2\gamma}$ decay. These two decays are therefore complimentary in searching for

²Note that when $\tan \beta$ is as large as m_t/m_b , the charged-Higgs-exchange induced operator of Eq. (62) could be as important as the m_t -enhanced operator of Eq. (57). This interaction gives $G_S = -G_P$, and contributes to the muon polarization in $K_{\mu 3}$ and $K_{\mu 2\gamma}$ decays with the same sign.

new sources of CP violation.

Generally speaking, G_P is suppressed by light fermion masses. In our SUSY calculation, G_P is proportional to m_μ . And G_R , being induced by W boson exchange only, is not subject to light fermion mass suppression. The relative enhancement factor $G_R/G_P \sim m_b/m_\mu$ can cause the dominance of a G_R interaction over a G_P interaction if the relevant mass scales and phases are of similar magnitude. This could turn out to be one advantage for measuring the muon polarization in $K^+ \rightarrow \mu^+\nu\gamma$ decay over that in $K^+ \rightarrow \pi^0\mu^+\nu$ decay, as $P_\mu^{\perp(\pi)}$ in the $K_{\mu 3}$ decay is expected to be comparable in size to the charged Higgs contribution to P_μ^\perp in the $K_{\mu 2\gamma}$ decay. For example, we take an optimistic value of $|V_{31}^{UR}V_{32}^{DL,R}| = 1/2$ for the squark family mixings and assume $\tan\beta = 50$ and a mass scale of 100 GeV for the charged Higgs and the gluino, the maximal effects for the $K_{\mu 2\gamma}$ decay are $|P_\mu^\perp| \leq 3 \times 10^{-2}$ for the W -induced G_R interaction and $|P_\mu^\perp| \leq 3 \times 10^{-3}$ for the charged Higgs induced G_P interaction. And these two contributions are larger by factors of $m_t m_b/m_s m_u \sim 10^6$ and $m_t/m_s \sim 10^3$ respectively than those in the absence of squark family mixings. Both limits could be accessible to the KEK E246 experiment and the proposed BNL experiment. However, the FSI effect is possibly as large as $\sim 10^{-3}$ and needs to be subtracted out. In comparison, the three-Higgs-doublet model gives comparable contributions to the muon polarization in $K_{\mu 3}$ and $K_{\mu 2\gamma}$ decays [14], and is therefore easily distinguished from SUSY models with a dominating W -exchange induced G_R interaction.

As the W -induced G_R interaction ($\propto V_{32}^{DR*}V_{31}^{UR}/M_{SUSY}^2$) and the charged-Higgs induced G_P interaction ($\propto V_{32}^{DL*}V_{31}^{UR}/m_H^2$) involve different squark mixing matrices and different mass parameters, the possibility of charged-Higgs-exchange dominance should not be discarded. For charged Higgs exchange, the m_t -enhanced effective interaction of Eq. (57) could have the largest effect on P_μ^\perp , and it also gives $G_S = G_P$. The resulting muon polarizations in $K_{\mu 3}$ and $K_{\mu 2\gamma}$ decays are comparable in size but opposite in sign. By contrast, the dominating effect in the three-Higgs-doublet model gives $G_S = -G_P$, and the muon polarizations are always comparable in size and have the same sign for the two decays [14].

Therefore, the three-Higgs-doublet model is again distinguishable from SUSY models with charged Higgs exchange dominance. However, when $\tan\beta$ is roughly as large as m_t/m_b , the m_b -suppressed four-Fermi operator of Eq. (62), which gives $G_S = -G_P$, could be as important as the m_t -enhanced operator of Eq. (57), and the prediction of the relative sign between $P_\mu^{\perp(\pi)}$ in the $K_{\mu 3}$ decay and P_μ^\perp in the $K_{\mu 2\gamma}$ decay would then be lost in this particular region of the SUSY parameter space.

Unlike the $K_{\mu 2\gamma}$ decay for which the branching ratio is about half of a per cent, the branching ratios for the radiative $D \rightarrow l\nu\gamma$ ($l = e, \mu$) and $B \rightarrow l\nu\gamma$ ($l = e, \mu, \tau$) decays are too tiny for measuring the transverse lepton polarization P_l^\perp at future τ -charm and B factories. On the other hand, due to kinematic suppressions of the interference amplitude and/or experimental technical difficulties in measuring the electron polarization, other radiative pion and kaon leptonic decays including $\pi^+ \rightarrow \mu^+\nu\gamma$, $\pi^+ \rightarrow e^+\nu\gamma$, and $K^+ \rightarrow e^+\nu\gamma$, are not as suitable for studying T violation at present time. For these reasons, the radiative $K_{\mu 2}$ decay is unique as a probe of new sources of CP violation. We have considered large squark family-mixings in supersymmetry, and found the polarization measurement in the $K_{\mu 2\gamma}$ decay and charged meson semileptonic decays at current and future meson factories to be very valuable for probing this region of SUSY parameter space.

ACKNOWLEDGMENTS

We would like to thank D. Bryman, K. Kiers, T. Numao, especially Y. Kuno for valuable conversations, and W.J. Marciano for suggesting the study of radiative kaon decay and for helpful correspondence. This work is partially supported by the Natural Sciences and Engineering Research Council of Canada.

REFERENCES

- [1] Y. Kuno, Nucl. Phys. B (Proc. Suppl.) **37A**, 87 (1994).
- [2] R. Adair *et al.*, muon polarization working group report, hep-ex/9608015.
- [3] M.K. Campbell *et al.*, Phys. Rev. Lett. **47**, 1032 (1981);
S.R. Blatt *et al.*, Phys. Rev. D **27**, 1056 (1983).
- [4] E. Golowich and G. Valencia, Phys. Rev. D **40**, 112 (1989).
- [5] A.R. Zhitnitskii, Yad. Fiz. **31**, 1024 (1980) [Sov. J. Nucl. Phys., **31**, 529 (1980)]
- [6] H.Y. Cheng, Phys. Rev. D **26**, 143 (1982);
R. Garisto and G. Kane, Phys. Rev. D **44**, 2038 (1991);
G. Belanger and C.Q. Geng, Phys. Rev. D **44**, 2789 (1991).
- [7] S. Weinberg, Phys. Rev. Lett. **37**, 657 (1976).
- [8] G.-H. Wu and J.N. Ng, TRI-PP-96-49, hep-ph/9609314.
- [9] E. Christova and M. Fabbrichesi, Phys. Lett. B **315**, 113 (1993).
- [10] W.J. Marciano, private communication, and in the Proceedings of "Workshop on Future Directions in Particles and Nuclear Physics at Multi-GeV Hadron Beam Facilities", BNL, 1993.
- [11] C.Q. Geng, Nucl. Phys. B (Proc. Suppl.) **37A**, 59 (1994).
- [12] M. Kobayashi and T. Maskawa, Prog. Theor. Phys. **49**, 652 (1973).
- [13] C.Q. Geng and S.K. Lee, Phys. Rev. D **51**, 99 (1995).
- [14] M. Kobayashi, T-T. Lin, and Y. Okada, Prog. Theor. Phys. **95**, 361 (1996).
- [15] D.A. Bryman *et al.*, Phys. Rep. **88**, 151 (1982).
- [16] J. Bijnens, G. Ecker, and J. Gasser, Nucl. Phys. **B396**, 81 (1993).
- [17] D.Yu. Bardin and E.A. Ivanov, Sov. J. Part. Nucl. **7**, 286 (1976), and references therein.
- [18] M. Leurer, Phys. Rev. Lett. **62**, 1967 (1989);
P. Castoldi, J.M. Frere and G. Kane, Phys. Rev. D **39**, 263 (1989);
H.Y. Cheng, Phys. Rev. D **28**, 150 (1983).
- [19] B.A. Campbell, Phys. Rev. D **28**, 209 (1983);
M.J. Duncan, Nucl. Phys. **B221**, 285 (1983);
J.F. Donoghue, H.P. Nilles, and D. Wyler, Phys. Lett. B **128**, 55 (1983);
L.J. Hall, V.A. Kostelecky, and S. Raby, Nucl. Phys. **B267**, 415 (1986);

- F. Gabbiani and A. Masiero, Nucl. Phys. **B322**, 235 (1989);
J.S. Hagelin, S. Kelley, and T. Tanaka, Nucl. Phys. **B415**, 293 (1994);
F. Gabbiani, E. Gabrielli, A. Masiero, and L. Silvestrini, Nucl. Phys. **B477**, 321 (1996).
- [20] M. Dine, R. Leigh, and A. Kagan, Phys. Rev. D **48**, 4269 (1993);
Y. Nir and N. Seiberg, Phys. Lett. B **309**, 337 (1993);
M. Leurer, Y. Nir, and N. Seiberg, Nucl. Phys. **B420**, 468 (1994).
- [21] N. Arkani-Hamed, H.-C. Cheng, and L.J. Hall, Phys. Rev. D **53**, 413 (1996); Phys. Rev. D **54**, 2242 (1996).
- [22] S. Dimopoulos and L.J. Hall, Phys. Lett. B **344**, 185 (1995);
R. Barbieri, L.J. Hall, and A. Strumia, Nucl. Phys. **B449**, 437 (1995).
- [23] Y. Grossman, H. Haber and Y. Nir, Phys. Lett. B **357**, 630 (1995).
- [24] R. Barbieri and G.F. Giudice, Phys. Lett. B **309**, 86 (1993);
R. Garisto and J.N. Ng, Phys. Lett. B **315**, 372 (1993);
Y. Okada, Phys. Lett. B **315**, 119 (1993);
N. Oshimo, Nucl.Phys. **B404**, 20 (1993);
M.A. Diaz, Phys. Lett. B **322**, 207 (1994);
F.M. Borzumati, Z.Phys. C **63**, 291 (1994);
S. Bertolini and F. Vissani, Z. Phys. C **67**, 513 (1995).

TABLES

TABLE I. Effects of different types of interactions on P_μ^\perp in the $K_{\mu 2\gamma}^+$ decay. The G_L and G_R are effective operators containing respectively left-handed and right-handed quark currents. The sign and magnitude of δ is model dependent, and it also varies from one type of interaction to another. A \checkmark denotes a non-zero contribution to the muon polarization.

	δ_{IB}	δ_V	δ_A	P_{IB-V}^\perp	P_{IB-A}^\perp	P_μ^\perp
G_S	0	0	0	0	0	0
G_P	δ	0	0	\checkmark	\checkmark	\checkmark
G_V	0	δ	0	\checkmark	0	\checkmark
G_A	δ	0	δ	\checkmark	0	\checkmark
G_L	δ	δ	δ	0	0	0
G_R	δ	$-\delta$	δ	\checkmark	0	\checkmark

FIGURES

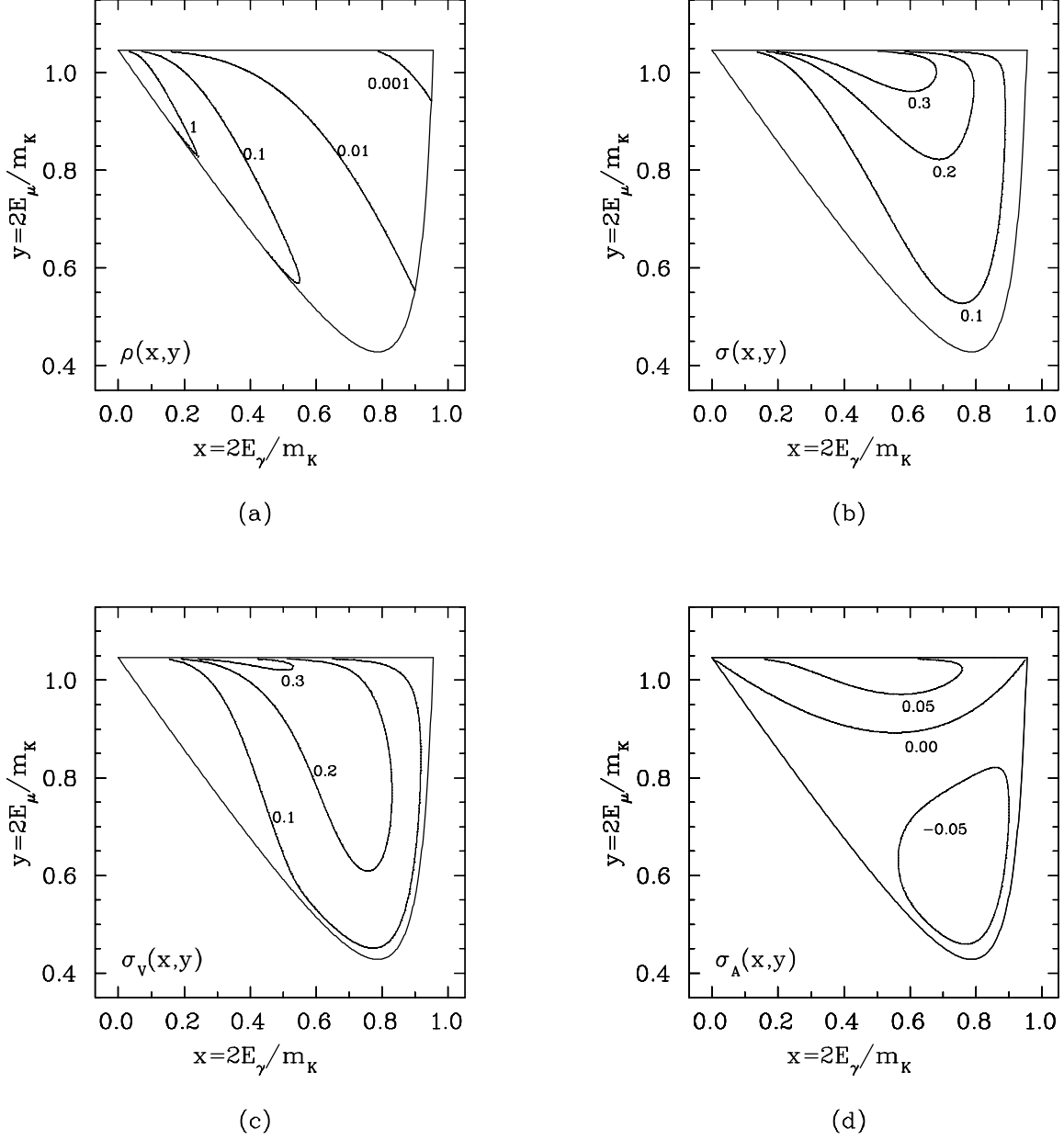


FIG. 1. Contour plots of the normalized Dalitz density $\rho(x,y)$ (a), and the transverse muon polarization functions $\sigma(x,y)$ (b), $\sigma_V(x,y)$ (c), and $\sigma_A(x,y)$ (d) in the $K^+ \rightarrow \mu^+ \nu \gamma$ decay.

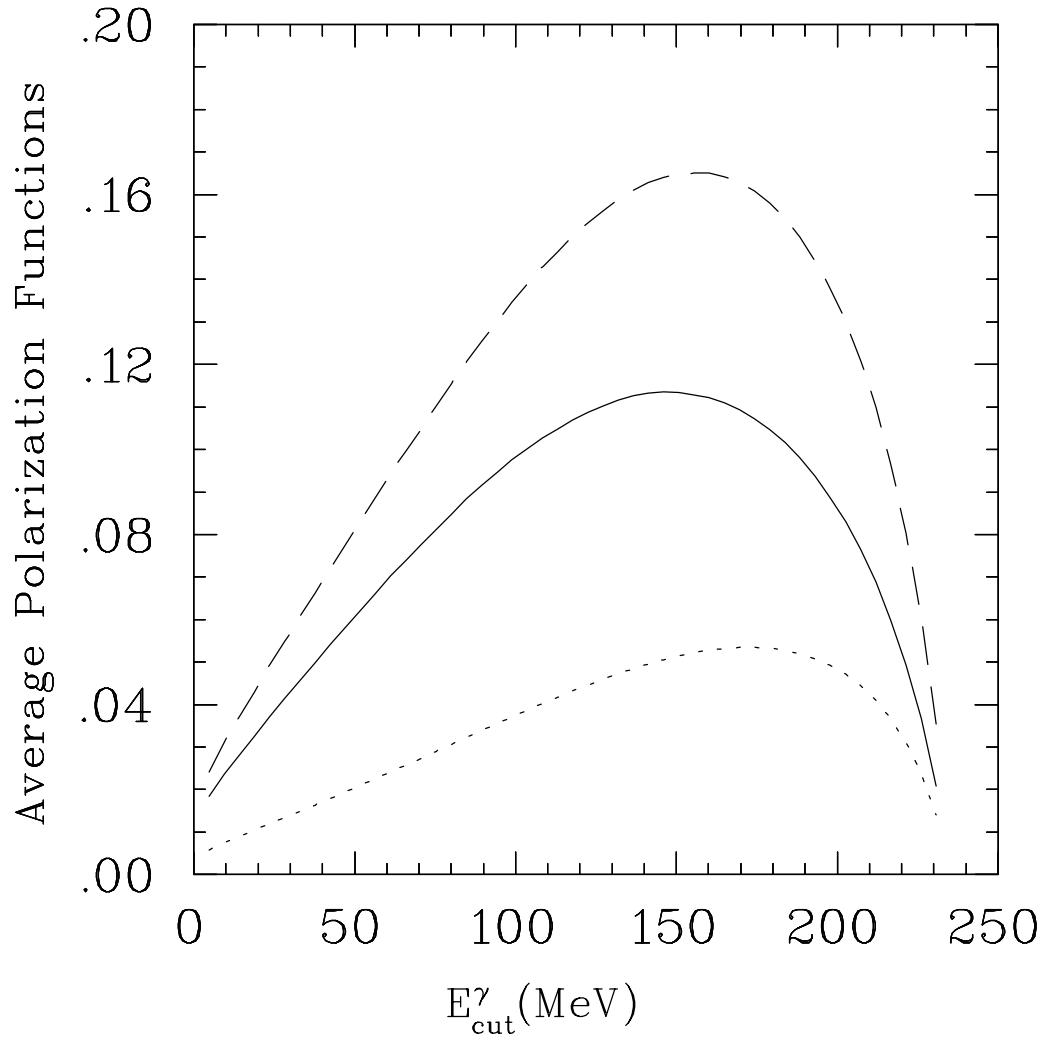
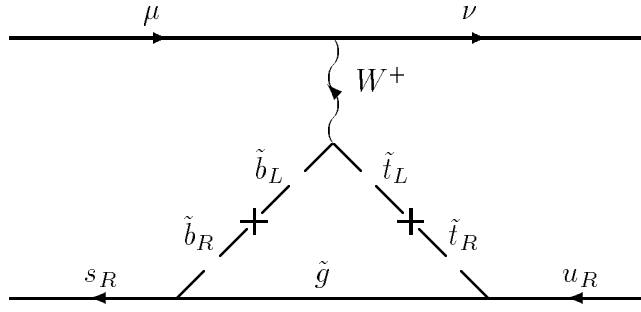
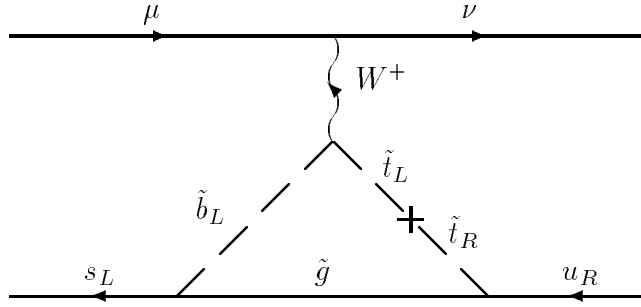


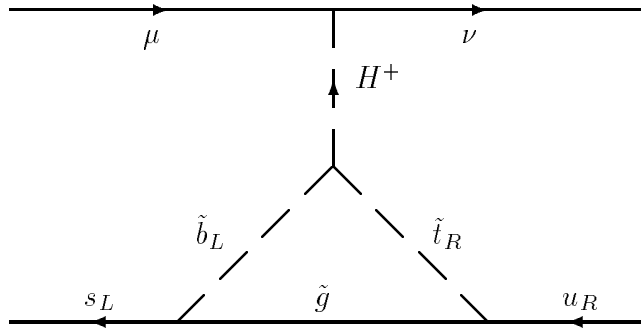
FIG. 2. The averaged transverse muon polarization functions vs. the soft photon energy cut E_{cut}^γ for the $K^+ \rightarrow \mu^+ \nu \gamma$ process: $\bar{\sigma}$ (solid line), $\bar{\sigma}_V$ (long-dashed line), and $-\bar{\sigma}_A$ (short-dashed line).



(a)



(b)



(c)

FIG. 3. Supersymmetry diagrams for (a) the W -exchange induced effective G_R interaction (see Eq. (43)), (b) the W -exchange induced effective G_P interaction (see Eqs. (47) and (52)), and (c) the H^+ -exchange induced effective G_P interaction (see Eq. (57)).

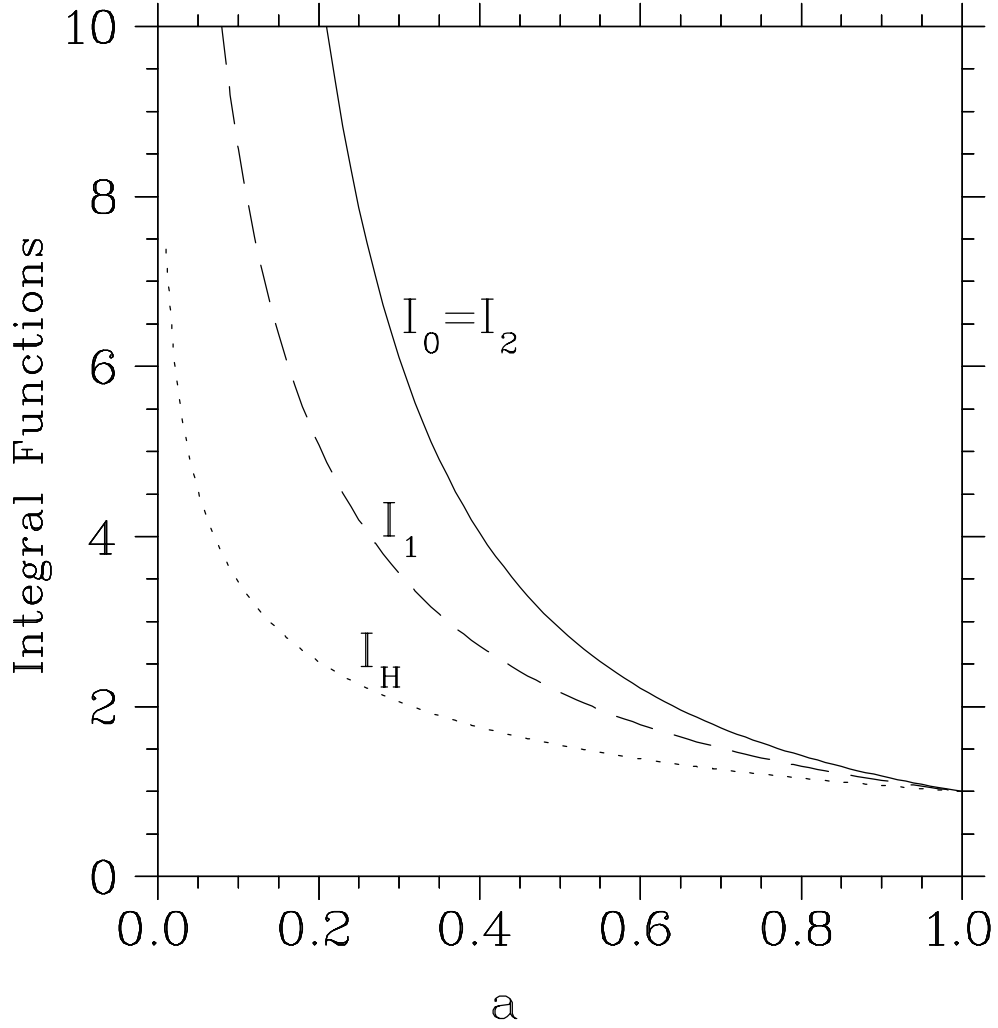


FIG. 4. The integral functions vs. the parameter $a = \frac{m_i^2}{m_g^2} = \frac{m_b^2}{m_g^2}$ for I_0 (Eq. (45)) and I_2 (Eq. (51)) (solid line), I_1 (Eq. (50)) (long-dashed line), and I_H (Eq. (59)) (short-dashed line).